Genetic diversity and evolution of Hantaan virus in China and its neighbors

Genetic diversity and evolution of Hantaan virus

Naizhe Li[a], Aqian Li[a], Yang Liu[a], Wei Wu[a], Chuan Li[a], Dongyang Yu[b], Yu Zhu[b], Jiandong Li[a], Dexin Li[a], Shiwen Wang[a,c,], Mifang Liang[a,c,*]*

[a] Key Laboratory of Medical Virology and Viral Diseases, Ministry of Health of People's Republic of China, National Institute for Viral Disease Control and Prevention, Chinese Center for Disease Control and Prevention, Beijing, 102206, China.

[b] Department of Microbiology, Anhui Medical University, Hefei, 230032, China.

[c] Center for Biosafety Mega-Science, Chinese Academy of Sciences, Beijing 100049, P. R. China

*Address correspondence to Shiwen Wang, wangsw@ivdc.chinacdc.cn.

*Address correspondence to Mifang Liang, liangmf@ivdc.chinacdc.cn.

Abstract

Backgroud

Hantaan virus *(HTNV)*, as one of the pathogenic hantaviruses of HFRS, has raised serious concerns in Eurasia. China and its neighbors, especially Russia and South Korea, are seriously suffered HTNV infections. Recent studies reported genetic diversity and phylogenetic features of HTNV in different parts of China, but the analyses from the holistic perspective are rare.

Methodology and Principal Findings

To better understand HTNV genetic diversity and dynamics, we analyzed all available complete sequences derived from the S and M segments with bio-informatic tools. Our study revealed 11 phylogroups and sequences showed obvious geographic clustering. We found 42 significant amino acid variants sites and 18 of them located in immune epitopes. Nine recombination events and seven reassortment isolates were deteced in our study. Sequences from Guizhou were highly genetic divergent, characterized by the emergence of multiple lineages, recombination and reassortment events. We found that HTNV probably emerged in Zhejiang about 1,000 years ago and the population size expanded from 1980s to 1990s. Bayesian stochastic search variable selection analysis revealed that Heilongjiang, Shaanxi and Guizhou played important roles in HTNV evolution and migration.

Conclusions/Significance

These findings reveal the original and evolution features of HTNV which might assist in understanding Hantavirus epidemics and would be useful for disease prevention and control.

Author summary

Hemorrhagic Fever with Renal Syndrome (HFRS) and Hantavirus Pulmonary Syndrome (HPS) are endemic zoonotic infectious diseases caused by hantaviruses that belong to the Family Bunyaviridae. Hantaviruses have gained worldwide attention as etiological agents of emerging zoonotic diseases, with fatality rates ranging from <10% up to 60%. However, our knowledge about the emergence and evolution of HTNV is limited. To get more information about HTNV genetic diversity and phylogenetic features in holistic perspective, we investigated the genetic diversity and spatial distribution of HTNV using all available whole genomic sequences of S and M segments. We also gain insights into the genetic diversity and spatial-temporal dynamics of HTNV. These data can augment traditional approach to infectious disease surveillance and control.

Keywords Hantaan virus; recombination; Bayesian phylogenetics; Viral phylodynamic; Spatial transmission

Introduction

Hantaviruses have gained worldwide attention as etiological agents of emerging zoonotic diseases, namely hemorrhagic fever with renal syndrome (HFRS) in Eurasia and hantavirus cardiopulmonary syndrome (HCPS) in Americas, with fatality rates ranging from <10% up to 60%[1]. Among all the countries, China is the most seriously affected one which account for over 90% of the total HFRS cases around the world[2, 3]. It has been reported that the HFRS death rate in China was 2.89% during the years 1950– 2014[4]. Although a declining HFRS trend has been observed at a global scale in China, there still exist certain local regions that continue to display increasing HFRS trends [5]. However, the causative agent of the disease remained unknown until the early 1970s, when Lee et al. reported on Hantaan virus (HTNV), present in the lungs of its natural reservoir, the striped field mouse (Apodemus agrarius)[6].

Hantaan virus, as one of the pathogenic hantaviruses of HFRS, is a member of genus Orthohantavirus, family Hantaviridae in the order Bunyavirales. The virus genome consists of three separate segments of negative-stranded RNA referred to as small (S), medium (M), and large (L) segments, which encode nucleocapsid protein (NP), two envelope glycoproteins (Gn and Gc) and viral RNA-dependent RNA polymerase (RdRP), respectively[7]. Recent studies[8-10] reported genetic diversity and phylogenetic features of HTNV in different

parts of China, but the analyses from the holistic perspective are rare. Also, the mechanisms underlying the emergence and evolution of HTNV are poorly understood. Understanding the phylogenetic factors contributing to HTNV transmission has important implications for our understanding of its epidemiology and providing insights about the surveillance and outbreak predictions or preparation.

In this study, we focused on the genetic diversity and evolution history of Hantaan virus. Whole-genome sequences were analyzed with bio-information tools. The results revealed the phylogenetic relationships among HTNV strains with both Bayesian and Maximum Likelihood methods. To deduce geographic origins and migration patterns of HTNV epidemics, BEAST software was used in this study. Furthermore, the recombination and reassortment events were also detected.

Materials and methods.

1. Sequence dataset

All the complete S gene and M gene sequences of Hantaan orthohantavirus deposited until June 2019 were collected from Virus Pathogen Database and Analysis Resource (ViPR, www.viprbrc.org). Only one sequence was retained for the identity sequences with the same strain names. It should be mentioned that sequences from Shandong

104 province (accession no. KY639536-KY639711) were not defined as
105 HTNV by ViPR and Genebank but can be organized in Hantaan
106 orthohantavirus (see below). These sequences were still analyzed in this
107 study. All the sequences were aligned using MAFFT version7[11] with
108 default settings followed by manual refinement. The coding sequences
109 were retained and used for the following analyses[12].

110 2. Recombination detection

111 As recombination seriously affects phylogenetic inference, the whole
112 dataset was tested for the presence of recombination signals using
113 RDP4[13]. RDP, GENECONV, Maximum Chi-squared, Chimaera,
114 Bootscan, Sister Scanning and 3Seq were used Only events with P
115 values<0.01 that were confirmed by four or more methods were considered
116 as recombination.

117 3. Phylogenetic analyses and amino acid substitution analyses

118 To reduce the potential bias, the recombination segments were removed
119 from the datasets firstly. The phylogenetic relationships of the complete S
120 and M gene sequences were estimated using a Bayesian Markov Chain
121 Monte Carlo (MCMC) method as implemented in MrBayes v3.2.2[14] and
122 a maximum-likelihood (ML) phylogenetic inference as implemented in
123 IQ-TREE v1.6.8[15]. Dobrava virus (DOBV), Puumala virus (PUUV), Sin
124 Nombre virus (SNV) and Thottapalayam virus (TPMV) were designated

as outgroup.

For Bayesian MCMC analysis, the suitability of substitution models for our datasets were assessed using jModelTest v2.1.10[16], which performed a statistical model selection procedure based on the Akaike Information Criterion (AIC). It identified the best fitting substitution model GTR+Γ for both datasets of complete S and M gene sequences. The MCMC settings consisted of two simultaneous independent runs with four chains each, which were run for 20 million generations and sampled every 200 generation with a 25% burn-in.

For maximum-likelihood analysis, the best-fitting nucleotide substitution model that minimizes the Bayesian Information Criterion (BIC) score was selected by ModelFinder[17], implemented in IQ-TREE. A ML tree was constructed using the best-fitting nucleotide the substitution model, and statistical robustness of the branching order within the tree was assessed using ultrafast bootstrap support values[18] (1000 replicates) and the SH-like approximate likelihood ratio test[19] (SH-aLRT) (5000 replicates). The trees were visualized in FigTree v1.4.4 (http://tree.bio.ed.ac.uk/software/figtree/).

Metadata-driven comparative analysis tool (meta-CATS) supplied by ViPR was used to analyze the variation of amino acid between the different phylogenetic groups, host and sample collection years. The P value

146 threshold was set to 0.05. If a specific amino acid exists only in one species
147 or one group but not in other species or group, this amino acid is considered
148 a 'significant amino acid' marker (or synapomorphy).

149 4. Coalescent and evolution analyses

150 Complete S gene sequences were used to deduce the evolution history
151 of Hantaan virus. To avoid potential biases due to sampling heterogeneity,
152 the dataset was reduced using CD-HIT[20] by clustering together
153 sequences with a nucleotide sequence identity threshold of 99%. Temporal
154 evolutionary signal in ML tree was evaluated by using TempEst[21] v1.5.1,
155 which plots sample collection dates against root-to-tip genetic distances
156 obtained from the ML phylogeny tree.

157 The tMRCA, substitution rates, and evolution history were estimated
158 using a Bayesian serial coalescent approach implemented in BEAST
159 v1.10.4[22]. jModelTest v2.1.10. was used to determine the model of
160 nucleotide substitution that best fit the dataset, and the dataset was
161 subsequently run using GTR+I+Γ. Both strict and relaxed (uncorrelated
162 exponential and uncorrelated lognormal) molecular clocks were used for
163 the analysis combined with different tree prior (Constant Population size,
164 GMRF Bayesian Skyride, Bayesian Skyline were used in this study).
165 Time- scale was inferred using an informative substitution rate interval

(1.0×10^{-4} to 1.0×10^{-3} substitutions/site/year) previously estimated for the N gene of rodent-borne hantavirus[23]. Models were compared pairwise by estimating the Log marginal likelihood via path sampling (PS) and stepping stone (SS) analysis[24-26]. For each model, an MCMC was run for 100 million generations, sampling every 10,000 steps. Posterior probabilities were calculated using the program Tracer1.7 after 10% burn-in. The results were accepted only if the effective sample sizes (ESS) exceeded 200.

The selected molecular clock/demographic model (strict clock with Bayesian skyline prior in this study) was then used for the Bayesian phylogeographic inference based on the continuous-time Markov Chain (CTMC) process over discrete sampling locations to estimate the diffusion rates among locations, with Bayesian stochastic search variable selection (BSSVS). The MCMC was run for 200 million generations, with sampling every 20,000 generations. Only parameter estimates with ESS values exceeding 200 were accepted. A maximum clade credibility (MCC) tree with the phylogeographic reconstruction was selected from the posterior tree distribution after a 10% burn-in using the Tree Annotator v 1.10 and was manipulated in FigTree v1.4.4. The migration routes were visualized using SPREAD3[27]. Migration pathways were considered to be important when they yielded a Bayes factor greater than

15 and when the mean posterior value of the corresponding was greater than 0.50. Bayes factors were interpreted according to the guidelines of Kass and Raftery[28].

Results

1. HTNV sequences dataset

A total of 225 complete S gene sequences and 180 complete M gene sequences from 238 HTNV strains were contained in the dataset. The sampling dates of the sequences ranged from 1976 to 2017. According to the sample collection area, 18 regions were defined, including Russia, South Korea and 16 provinces of China (Fig 1A). The samples were collected from 9 kinds of hosts, including *Apodemus agrarius, Apodemus peninsulae, Rattus norvegicus, Mus musculus, Nivienter confucianus, Tscherskia triton, Mirotus fortis, Crocidura russula, and Homo sapiens.* The details of the sequences are shown in Fig 1.

Fig 1. The details of the datasets.

(A) The number of isolates collected from different regions. The bars were colored in different sampling years. (AH, Anhui; GD, Guangdong; GZ, Guizhou; HB, Hubei; HLJ, Heilongjiang; HN, Hunan; JL, Jilin; JS, Jiangsu; JX, Jiangxi; LN, Liaoning; RUS, Russia; SC, Sichuan; SD, Shandong; SK, South Korea; SX, Shaanxi; TJ, Tianjin; UN, Unknown; YN, Yunnan; ZJ, Zhejiang;) (B) The number of isolates collected from different hosts. (Aa,

208 *Apodemus agrarius; Ap, Apodemus peninsulae; Rn, Rattus norvegicus; Mm,Mus musculus;*
209 *Nc, Nivienter confucianus; Tt, Tscherskia triton; Mf, Mirotus fortis; Cr, Crocidura russula;*
210 *Hs, Homo sapiens.) The bars were colored in different regions. (C) The number of isolates*
211 *collected in different years.*
212
213 2. Recombination events detection
214 To reduce the potential bias, the recombination segments should be
215 removed from the datasets. Recombination events were detected among all
216 the 225 complete S gene sequences and 180 complete M gene sequences
217 from 238 HTNV strains collected in this study. The RDP analysis
218 suggested 9 recombination events in 6 HTNV isolates, and all the
219 recombination events were occurred in M gene segment (Table 1). Similar
220 recombination events were detected in three isolates (CGAa31MP7,
221 CGAa31P9, CGHu2). All this three isolates were collected during 2004 to
222 2005 in Guizhou province[8]. It would imply that these isolates have the
223 same ancestor which has experienced recombination before. Although
224 only 5 methods suggested the recombination event occurred in strain
225 JN131026, the p-values were all lower than 0.01. Considering the
226 consensus score is higher than 0.6 (0.646), we defined it as a recombinant
227 isolate. P-values of the event tested in strain A16 were in high credible
228 level.

229

230 Table 1. Recombination events detected in all HTNV sequences

Events	Recombinant	Segment	Beginning	Ending	Major Parent	Minor Parent	Method(s) by which breakpoint was detected in RDP4
1	CGAa31MP7	M	1756	1916	CGRni1	CGRn15	RDP/GENECONV/MaxChi/Chimaera/Bootscan/SisScan/3Seq
2	CGAa31MP7	M	2315	3402	Q32	CGRn2616	RDP/GENECONV/MaxChi/Chimaera/Bootscan/SisScan/3Seq
3	CGAa31P9	M	1756	1916	CGRni1	CGRn15	RDP/GENECONV/MaxChi/Chimaera/Bootscan/SisScan/3Seq
4	CGAa31P9	M	2315	3402	Q32	CGRn2616	RDP/GENECONV/MaxChi/Chimaera/Bootscan/SisScan/3Seq
5	CGHu2	M	1756	1916	CGRni1	CGRn15	RDP/GENECONV/MaxChi/Chimaera/Bootscan/SisScan/3Seq
6	CGHu2	M	2315	3402	Q32	CGRn2616	RDP/GENECONV/MaxChi/Chimaera/Bootscan/SisScan/3Seq
7	CGRn93P8	M	2386	3402	CGRn93MP8	CGHu2	RDP/GENECONV/MaxChi/Chimaera/Bootscan/SisScan/3Seq
8	JN131026	M	1413	2181	JN131027	158577	MaxChi/Chimaera/Bootscan/SisScan/3Seq
9	A16	M	2214	3402	H8205	SN7	RDP/GENECONV/MaxChi/Chimaera/Bootscan/SisScan/3Seq

232 3. Phylogenetic analyses and amino acid substitution analyses

233 The recombination isolates were excluded first. Our phylogenetic
234 analysis showed that 11 groups were defined with S segment, each with
235 high degree of support (Fig 2). The isolates were mainly clustered
236 together by region. The isolates from South Korea all belonged to Group
237 A. All the sequences from Jiangsu province and one strain from Sichuan
238 (S85_46) province clustered in Group A with sequences from South
239 Korea. Group B was formed with sequences collected from Russia and
240 the Northeast of China. The isolates collected in Shaanxi were all
241 clustered in Group C except one strain, 84FLi, which was isolated years
242 ago in 1984. All the three isolates from Hubei constituted group D and
243 all the isolates from Shandong clustered as a subgroup in Group E. The
244 other subgroup of Group E contains strains collected from Anhui,
245 Hunan, Guizhou, Shaanxi, Sichuan and Yunnan. The isolates collected
246 from Zhejiang constitute Group G and Group H, except one strain, N8,
247 which included in Group J. Group J also contains isolates from Jiangxi
248 and Liaoning with the sequences of each region clustered together.
249 Group K was formed with three isolates from Russian. We can notice
250 that the isolates collected from Guizhou province were highly divergent.
251 They dispersed in Group B, C, E, F and I. It indicates that HTNV has
252 spread in Guizhou for a long period.

Fig 2. Phylogenetic trees of S gene and M gene reconstructed by MyBayes.

Posterior node probabilities/SH-like approximate likelihood values/ultrafast bootstrap values for major nodes (black circles) are shown. Splits network analysis of HTNV was also shown.

There were 10 distinct phylogroups in M gene tree. The structure of phylogenetic tree reconstructed by M gene was identity with S gene tree except for 7 isolates (CGRn15, CGAa2, CGAa75, CGRn2616, CGRn2618, CGRn45, CGHu3) derived from Guizhou province. They were classified into Group I but in the S gene tree they were included in Group C. It suggested that reassortment events occurred in these strains. The branching order within the lineages differed in S and M trees, which indicates the different evolutionary history between the M and S segments.

We analyzed the variation of amino acid between the different phylogenetic groups. We noticed that 5 amino acid sites on NP gene and 37 on Gn/Gc gene were group specific and could be markers to distinguish different groups (Fig 3). No significant variant was found at the highly conserved pentapeptide motif WAASA, which is thought the cleavage of the GPC polypeptide into the Gn and Gc transmembrane proteins[29]. To determine if any of these amino acid sites were located in any known immune epitopes, we compared these significant positions against information about experimentally determined immune epitopes curated by

the IEDB. We found a total of 18 positions that were located in known immune epitopes (Table 2). No significant amino acid marker was found among different hosts or collected times.

Fig 3. The 'significant amino acid marker' of each group. *The specific amino acid sites of each group were marked by different colors.*

Table2. The significant sequence variations' location on immune epitopes

Protein	Variation Site	*Epitopes*			
		Epitope ID	Description	Starting Position	Ending Position
NP	179	164302	NGIRKPKHLYVSLPN	169	183
	296	807	AEAAGCSMI	288	296
	334	17746	FSILQDMRNTIMASK	332	346
		149047	FSILQDMRNTI	332	342
Gn	8, 9	742143	VMASLVWPV	8	16
	209	567849	IVCFFVAV	208	215
	216	77254	K216, G217		
	218	77257	N218, L415		
	501	568239	PAITFIIL	499	506

Gc	664	743275	GVGSVPMHTDLELDF	663	677
	690	743113	FSLTSSSKYTYRRKL	677	691
		743694	KYTYRRKLTNPLEEA	684	698
	700, 701, 703	743887	LTNPLEEAQSIDLHI	691	705
		742696	AQSIDLHIEIEEQTI	698	712
	963	742777	DHINILVTKDIDFDN	950	964
		40611	LVTKDIDFD	955	963
	978	744025	NLGENPCKIGLQTSS	964	978
		743579	KIGLQTSSIEGAWGS	971	985
		744567	SIEGAWGSGVGFTLT	978	992
	1001	744698	TCLVSLTECPTFLTS	992	1006
		59502	SLTECPTFL	996	1004

		742922	ECPTFLTSIKACDK A	999	1013
	1042	743186	GKGGHSGSTFRC CHG	1034	1048
		744680	STFRCCHGEDCSQ IG	1041	1055
	1054	743149	GEDCSQIGLHAAA PH	1048	1062

4. The coalescent analyses and evolution of HTNV

To avoid potential biases in the phylogeographic reconstructions due to sampling heterogeneity, we obtained a "non-redundant" subset including 51 clusters. In order to make our dataset to represent all the 15 regions (there was no sequence with exact collected year from Anhui, Sichuan and Guangdong), isolate E142, Hunan03 and JS10 were added in the dataset. Temporal evolutionary signal analyses showed a positive correlation between genetic divergence and sampling time. The strict clock with Bayesian skyline prior model yielded a higher log marginal likelihood than the others, indicating the best fit model for our dataset (Table S1).

The results of our Bayesian phylogenetic analysis showed that HTNV probably first emerged in Zhejiang province of China (root posterior

292 probability = 0.29), with a most recent common ancestor in 1198 (95%
293 credibility interval 593-1591; Fig 4A). The root posterior probability of
294 Jiangxi, Shaanxi, Guizhou and Heilongjiang were also in higher levels. The
295 MCC tree of HTNV showed four obviously two separate clusters. One was
296 composed of isolates from the northeast of China and its surroundings, and
297 the other was composed of isolates from the south and middle of China (Fig
298 4B). These indicated HTNV has been evaluating in China respectively for
299 a long time. Reconstruction of the demographic history, using the extended
300 Bayesian skyline plot, revealed that the HTNV population size was
301 relatively constant from 1500 to 1970s, then expanded between 1980s and
302 1990s, and stayed steady from 2000 until now (Fig 3B). The mean
303 substitution rate of 2.0427×10^{-4} substitution/site/year, with a 95% HPD
304 that ranged from 1.0001×10^{-4} to 3.2076×10^{-4} was estimated.

305 **Fig 4. The MCC tree, root state posterior probabilities and effective**
306 **population sizes of Hantaan virus.**

307 *(A) MCC tree showing the evolutionary relationships and timescale of HTNV. Branch*
308 *colors denote inferred location states, as shown in the legend. The most recent common*
309 *ancestor and 95% credibility intervals are shown near the node. (B) The root state*
310 *posterior probabilities for the different regions. (C) Bayesian skyline plot showing*
311 *population size through time for HTNV. Highlighted areas correspond to 95% HPD*
312 *intervals.*

313 The spatiotemporal linkage of HTNV is shown in Fig 5. Significant
314 location transitions were found mainly in two regions, the northeast and the
315 middle of China (Fig 5A). It indicated that Heilongjiang may be the
316 radiation center of the northeast regions of China and the surrounding
317 countries. Significant migration events were found from Heilongjiang to
318 Liaoning and Fareast of Russia. The migration from Heilongjiang to
319 Khabarovsk was detected in high credible level (Bayes factor = 163.0).
320 Shaanxi was assumed as the radiation center of the middle of China. Virus
321 migration from Shaanxi to Tianjin, Yunnan and Guizhou were observed.
322 The number of observed sate changes pinpointed Shaanxi as the main
323 source of HTNV epidemics in China, at least in the middle of China, and
324 Heilongjiang as the dominating source of HTNV in northeast of China (Fig
325 5B).

326 **Fig 5. Reconstructed phylogeographic linkage and the total number of**
327 **location state transitions of Hantaan virus.**

328 *(A) The phylogeographic linkage constructed reconstruction of the HTNV using BEAST.*
329 *Thickness of lines represents the relative transmission rate between two regions. The*
330 *map was created by SpreadD3 software and the geographic data were provided by the*
331 *Natural Earth (*https://www.naturalearthdata.com/*). (B) Histogram of the total number*
332 *of location state transitions inferred from the HTNV dataset.*

333

Discussion

In this study, we used all the whole-genome sequences of segment S and M obtained from ViPR to analyses the genetic diversity and evolution of HTNV. Our analyses show that the HTNV can be divided into 11 groups. We named the groups based on the S tree for NP gene is more stable and more sequences are available. The isolates were geographic clustering. Sequences obtained from the same geographic area clustered together. It's worth noting that sequences from Guizhou are more diverse. We will discuss this later.

A total of 42 significant amid acid variant sites were found among the different groups. We noticed more significant variants in Group I. Isolates contained in Group I were all from Guizhou. The collection dates were during 1980s to 2000s. It also indicated a high genetic diverse of Hantaan virus in Guizhou. 18 significant amid acid variant positions were found located at known immune epitopes. Experimentation is needed to determine if peptides containing these residues can confers escape or can be used to develop serotype-specific reagents for serology-based diagnostics. None significant amino acid marker was found among different hosts and periods, demonstrating that geographic region is the mainly factor affecting the genetic diversity of HTNV. The different topologies indicate the different evolutionary history between the M and S

355 segments, which was also found in others studies[30, 31].

356 Our analyses showed that both reassortment and recombination play
357 important role in HTNV evolution. A number of studies have revealed
358 that genetic reassortment can occur between the arthropod-borne members
359 of the Bunyavirales naturally or experimentally[32-37]. We found 7
360 reassortment events occurred in M segments which is consistent with Zou,
361 et al[8]. We found 9 recombination events in our study. All the
362 recombination events were occurred in segment M. The reassortment and
363 recombination events found in Gn/Gc envelope glycoproteins were
364 consistent with their functional roles in the viral escape from
365 immunological responses. It should be notice that recombinant A16,
366 isolated in Shaanxi, has both major parent, H8205, and minor parent,
367 SN7. Strain H8205 has been classified into Amur virus, which indicates
368 recombination occurred across different species in hantavirus. Strain SN7
369 was isolated in Sichuan, which implies the relationship of the evolution of
370 HTNV between Shaanxi and Sichuan. The evidences of recombination
371 have been reported for TULV[38] and PUUV[39], even the recombination
372 in hantavirus is rare[40].

373 We investigated the evolution and migration of HTNV in China and
374 its surrounding countries using Bayesian phylogeographic inference. Our
375 phylogenetic analyses placed the root of the tree for HTNV in Zhejiang

with strong support (Fig 3B). But no migration event was found from Zhejiang to other regions. It may result from the lack of whole-genomic data from Zhejiang and its surrounding areas. Markov jump estimates between different locations pinpointed Heilongjiang as an important source of HTNV epidemics in northeast of China and far east of Russia. This finding may explain the high endemic in this area since 1931, when HFRS was first recognized in northeast of China[41, 42]. Similar pattern, Shaanxi was recognized as the origin of HTNV spread in middle of China. These can be explained by a scenario in which the virus was first introduced into these areas, then it expanded there. But the transmission sources to Heilongjiang and Shaanxi is still unclear.

Our analyses show the high diversity of isolates from Guizhou province. Phylogenetic analyses show that isolates collected from Guizhou province clustered in Group B, C, F, I. All the reassortment events and 7 of 9 recombination events occurred in Guizhou. We found same recombination pattern in strain CGAa31MP7, CGAa31P9 and CGHu2. All of these indicates that different sources of HTNV transmitted to Guizhou and evolved for a long time in this place[43, 44]. This assumption can be supported by our Markov jump estimate (Fig 4). Guizhou is more than 1,000 meters above sea level, adding to its rich mountainous topography and as much as 92.5% of the province's total

area is characterized by mountains. It makes A. agrarius, the main host of HTNV, sympatric in rural resident areas more common. The Hengduan Mountains region was hypothesized to have played an important role in the evolutionary history of Apodemus since the Pleistocene era[45, 46]. The Yunnan-Guizhou plateau, which connects and overlaps with the Hengduan Mountains region, is also thought to play an important role in HTNV evolution. But we only found acceptable migration from Shaanxi to Guizhou in our study. This may result from the lack of sequences in Guizhou. To reduce the bias, recombinant and reassortment isolates were removed. We also got rid of similar sequences with the identity more than 99%. So limited sequences from Guizhou were used for evolutionary and phylogeographic analyses. More gene information should be collected in order to know more about the HTNV evolution and spread in this area.

The most recent common ancestor of HTNV was determined about more than 800 years ago in our study. It's much earlier than the first HFRS patient was reported in the early 1930s[47]. But HFRS-like disease was described in Chinese writings about 1000 years ago[48], so we believe HTNV has spread in China for more than 1000 years. The most common recent ancestor by Ramsden[49] was 859 years before present (ybp) for all rodent hantaviruses estimated and 202 ybp for Murinae

viruses and a mean substitution rate for rodent hantavirus of 6.67×10^{-4} subs/site/year with a 95% HPD that ranged from 3.86×10^{-4} to 9.8×10^{-4} subs/site/year. Partial sequences (275 nt) were used in this study, which can explain the different in tMRCA estimation. A recent study[50] showed that the estimated rate of nucleotide substitutions for the N gene of all rodent-borne hantavirus was 6.8×10^{-4} subs/site/year, which is similar to 6.67×10^{-4} subs/site/year. Our results implied HTNV evolved in a lower speed compared to the other rodent-borne hantaviruses. The estimated rate of nucleotide substitutions of DOBV and PUUV, 3×10^{-4} and 5.5×10^{-4} subs/site/year separately, supporting our hypothesis[23].

The relatively recent origin of HTNV apparently contradicts the viral-host codivergence theory. Previous estimates of evolutionary dynamics in hantaviruses were based on the critical assumption that the congruence between hantavirus and rodent phylogenies reflects codivergence between these 2 groups since the divergence of the rodent genera Mus and Rattus, approximately 10 to 40 MYA, which indicates a mean substitution rate in the range of 10^{-8} subs/site/year[39, 51, 52]. However, the observation of host–pathogen phylogenetic congruence does not necessarily indicate codivergence. Phylogenetic congruence between a parasite and its host can also arise from delayed cladogenesis, where the parasite phylogeny tracks that of the host but without temporal association[53]. This could

occur if hantaviruses largely evolve host associations by cross-species transmission and related species tend to live in the same area, in which case a pattern of strong host–pathogen phylogenetic congruence could be observed in the absence of codivergence. Our evolutionary rates were estimated directly from primary sequence data sampled at known dates so that they more closely reflect the evolutionary changes undergone by the virus, at least in the short term. And with a mean substitution rate that is closer to other RNA virus, we consider our results is more reliable than codivergence theory.

Our demographic analyses revealed that HTNV population had expanded from 1980s to 1990s. As HTNV is a kind of rodent-borne virus, the population size of HTNV is relevant to rodents' population. Previous studies have revealed that climatic factors can influence HFRS transmission through their effects on the reservoir host (mostly rodents of the family Muridae) and environmental conditions[54-56]. It's reported that that global annual average temperatures increased by more than 1.2°F (0.7°C) from 1986 to 2016, relative to temperatures seen from 1901 to 1960[57]. Global warming may affect rodent winter survival through winter temperatures by a complicated process, and it may also influence the magnitude of HFRS outbreaks through summer climatic conditions (both temperature and rainfall). Additionally, as global climate change

accelerates, the amount of annual rainfall increased accurately[58]. Moreover, agriculture improved rapidly in China at the same period, leading to more available food, which is fit for the reproduction of rodents. The steady effective population from 2000 until now is benefit from the successful strategy for HTNV prevention in China.

However, some cautions must be taken when interpreting our results. We have estimated the genetic diversity age based only on N gene sequences, the evolution rate of HTNV may be underestimated. For the Gn/Gc envelope glycoproteins are more diverse and considered evolves in a higher speed. Furthermore, there may be geographic biases due to the unbalanced of sequences collecting region. The lack of whole-genome sequences in some region may result in the lacking of knowledge about HTNV migration. In addition, lack of sequences of L gene can be obtained now. More gene information should be collected and shared to solve these problems.

In conclusion, our study revealed 11 groups of HTNV and 43 significant amino acid markers for different groups. Both recombination and reassortment events can be detected in HTNV. The origin and migration of HTNV were also shown by our analyses. And a steady effective population from 2000 until now indicated the successful strategy for HTNV prevention. Guizhou may play an important role in the

480 evolution and spread of HTNV. As the rodents' population and activity
481 influence the spread and increasing of HTNV. Rodents prevention and
482 control is an effective way to reduce the incidence of diseases. These data
483 provide important insights for better understanding the genetic diversity
484 and spatial-temporal dynamics of HTNV and would be useful for disease
485 prevention and control.

486

487 **Reference**

488

489 1. Papa A. Dobrava-Belgrade virus: Phylogeny, epidemiology, disease. Antiviral Research.
490 95(2):104-17. doi: 10.1016/j.antiviral.2012.05.011.
491 2. Khaiboullina S, Morzunov S, St. Jeor S. Hantaviruses: Molecular Biology, Evolution and
492 Pathogenesis. Current Molecular Medicine. 5(8):773-90.
493 3. Jonsson CB, Figueiredo LT, Vapalahti O. A global perspective on hantavirus ecology,
494 epidemiology, and disease. 2010;23(2):412-41.
495 4. Jiang H, Du H, Wang LM, Wang PZ, Bai XF. Hemorrhagic Fever with Renal Syndrome:
496 Pathogenesis and Clinical Picture. Frontiers in cellular and infection microbiology. 2016;6:1. Epub
497 2016/02/13. doi: 10.3389/fcimb.2016.00001. PubMed PMID: 26870699; PubMed Central PMCID:
498 PMCPMC4737898.
499 5. Lin H, Zhang Z, Lu L, Li X, Liu Q. Meteorological factors are associated with hemorrhagic fever

500 with renal syndrome in Jiaonan County, China, 2006–2011. International Journal of Biometeorology.
501 2014;58(6):1031-7. doi: 10.1007/s00484-013-0688-1.
502 6. Lee HW, Lee PW, Johnson KM. Isolation of the Etiologic Agent of Korean Hemorrhagic Fever.
503 The Journal of Infectious Diseases. 1978;137(3):298-308. doi: 10.1093/infdis/137.3.298.
504 7. Plyusnin A, Vapalahti O, Vaheri A. Hantaviruses: genome structure, expression and evolution.
505 The Journal of general virology. 1996;77 (Pt 11):2677-87. Epub 1996/11/01. doi: 10.1099/0022-
506 1317-77-11-2677. PubMed PMID: 8922460.
507 8. Zou Y, Hu J, Wang ZX, Wang DM, Li MH, Ren GD, et al. Molecular diversity and phylogeny
508 of Hantaan virus in Guizhou, China: Evidence for Guizhou as a radiation center of the present
509 Hantaan virus. Journal of General Virology. 2008;89:1987-97. doi: 10.1099/vir.0.2008/000497-0.
510 9. Zou Y, Hu J, Wang Z-x, Wang D-m, Yu C, Zhou J-z, et al. Genetic Characterization of
511 Hantaviruses Isolated from Guizhou , China : Evidence for Spillover and Reassortment in Nature.
512 2008;1041:1033-41. doi: 10.1002/jmv.
513 10. Zuo S-q, Li X-j, Wang Z-q, Jiang J-f, Fang L-q, Zhang W-H, et al. Genetic Diversity and the
514 Spatio-Temporal Analyses of Hantaviruses in Shandong Province, China. Frontiers in Microbiology.
515 2018;9:1-13. doi: 10.3389/fmicb.2018.02771.
516 11. Katoh K, Standley DM. MAFFT multiple sequence alignment software version 7:
517 improvements in performance and usability. Mol Biol Evol. 2013;30(4):772-80. doi:
518 10.1093/molbev/mst010. PubMed PMID: 23329690; PubMed Central PMCID: PMCPMC3603318.
519 12. Maes P, Klempa B, Clement J, Matthijnssens J, Gajdusek DC, Kruger DH, et al. A proposal

for new criteria for the classification of hantaviruses, based on S and M segment protein sequences. Infection, genetics and evolution : journal of molecular epidemiology and evolutionary genetics in infectious diseases. 2009;9(5):813-20. doi: 10.1016/j.meegid.2009.04.012. PubMed PMID: 19393771.

13. Martin DP, Murrell B, Golden M, Khoosal A, Muhire B. RDP4: Detection and analysis of recombination patterns in virus genomes. Virus Evol. 2015;1(1):vev003. doi: 10.1093/ve/vev003. PubMed PMID: 27774277; PubMed Central PMCID: PMCPMC5014473.

14. Ronquist F, Huelsenbeck JP. MrBayes 3: Bayesian phylogenetic inference under mixed models. Bioinformatics. 2003;19(12):1572-4. doi: 10.1093/bioinformatics/btg180.

15. Nguyen L-T, Schmidt HA, von Haeseler A, Minh BQ. IQ-TREE: A Fast and Effective Stochastic Algorithm for Estimating Maximum-Likelihood Phylogenies. Molecular Biology and Evolution. 2014;32(1):268-74. doi: 10.1093/molbev/msu300.

16. Posada D. jModelTest: Phylogenetic Model Averaging. Molecular Biology and Evolution. 2008;25(7):1253-6. doi: 10.1093/molbev/msn083.

17. Kalyaanamoorthy S, Minh BQ, Wong TKF, von Haeseler A, Jermiin LS. ModelFinder: fast model selection for accurate phylogenetic estimates. Nature Methods. 2017;14:587. doi: 10.1038/nmeth.4285

https://www.nature.com/articles/nmeth.4285#supplementary-information.

18. Hoang DT, Chernomor O, von Haeseler A, Minh BQ, Vinh LS. UFBoot2: Improving the Ultrafast Bootstrap Approximation. Molecular Biology and Evolution. 2017;35(2):518-22. doi:

10.1093/molbev/msx281.

19. Guindon S, Dufayard J-F, Lefort V, Anisimova M, Hordijk W, Gascuel O. New Algorithms and Methods to Estimate Maximum-Likelihood Phylogenies: Assessing the Performance of PhyML 3.0. Systematic Biology. 2010;59(3):307-21. doi: 10.1093/sysbio/syq010.

20. Huang Y, Niu B, Gao Y, Fu L, Li W. CD-HIT Suite: a web server for clustering and comparing biological sequences. Bioinformatics. 2010;26(5):680-2. doi: 10.1093/bioinformatics/btq003.

21. Rambaut A, Lam TT, Max Carvalho L, Pybus OG. Exploring the temporal structure of heterochronous sequences using TempEst (formerly Path-O-Gen). Virus Evolution. 2016;2(1). doi: 10.1093/ve/vew007.

22. Drummond AJ, Suchard MA, Xie D, Rambaut A. Bayesian Phylogenetics with BEAUti and the BEAST 1.7. Molecular Biology and Evolution. 2012;29(8):1969-73. doi: 10.1093/molbev/mss075.

23. Ramsden C, Melo FL, Figueiredo LM, Holmes EC, Zanotto PMA, Moreli ML, et al. High rates of molecular evolution in hantaviruses. Molecular Biology and Evolution. 2008;25:1488-92. doi: 10.1093/molbev/msn093.

24. Baele G, Lemey P, Bedford T, Rambaut A, Suchard MA, Alekseyenko AV. Improving the Accuracy of Demographic and Molecular Clock Model Comparison While Accommodating Phylogenetic Uncertainty. Molecular Biology and Evolution. 2012;29(9):2157-67. doi: 10.1093/molbev/mss084.

25. Baele G, Li WLS, Drummond AJ, Suchard MA, Lemey P. Accurate Model Selection of Relaxed Molecular Clocks in Bayesian Phylogenetics. Molecular Biology and Evolution. 2012;30(2):239-43.

560 doi: 10.1093/molbev/mss243.

561 26. Baele G, Lemey P. Bayesian evolutionary model testing in the phylogenomics era: matching
562 model complexity with computational efficiency. Bioinformatics. 2013;29(16):1970-9. doi:
563 10.1093/bioinformatics/btt340.

564 27. Bielejec F, Baele G, Vrancken B, Suchard MA, Rambaut A, Lemey P. SpreaD3: Interactive
565 Visualization of Spatiotemporal History and Trait Evolutionary Processes. Molecular Biology and
566 Evolution. 2016;33(8):2167-9. doi: 10.1093/molbev/msw082.

567 28. Gao F, Liu X, Du Z, Hou H, Wang X, Wang F, et al. Bayesian phylodynamic analysis reveals
568 the dispersal patterns of tobacco mosaic virus in China. Virology. 2019;528:110-7. doi:
569 10.1016/j.virol.2018.12.001. PubMed PMID: 30594790.

570 29. Lober C, Anheier B, Lindow S, Klenk HD, Feldmann H. The Hantaan virus glycoprotein
571 precursor is cleaved at the conserved pentapeptide WAASA. Virology. 2001;289(2):224-9. doi:
572 10.1006/viro.2001.1171. PubMed PMID: 11689045.

573 30. Kang HJ, Stanley WT, Esselstyn JA, Gu SH, Yanagihara R. Expanded host diversity and
574 geographic distribution of hantaviruses in sub-Saharan Africa. J Virol. 2014;88(13):7663-7. doi:
575 10.1128/JVI.00285-14. PubMed PMID: 24741077; PubMed Central PMCID: PMCPMC4054438.

576 31. Razzauti M, Plyusnina A, Henttonen H, Plyusnin A. Microevolution of Puumala hantavirus
577 during a complete population cycle of its host, the bank vole (Myodes glareolus). PLoS One.
578 2013;8(5):e64447. doi: 10.1371/journal.pone.0064447. PubMed PMID: 23717616; PubMed
579 Central PMCID: PMCPMC3661530.

580 32. Beaty BJ, Sundin DR, Chandler LJ, Bishop DH. Evolution of bunyaviruses by genome
581 reassortment in dually infected mosquitoes (Aedes triseriatus). Science (New York, NY).
582 1985;230(4725):548-50. Epub 1985/11/01. doi: 10.1126/science.4048949. PubMed PMID:
583 4048949.
584 33. Szabo R, Radosa L, Lickova M, Slavikova M, Heroldova M, Stanko M, et al. Phylogenetic
585 analysis of Puumala virus strains from Central Europe highlights the need for a full-genome
586 perspective on hantavirus evolution. Virus genes. 2017;53(6):913-7. Epub 2017/07/01. doi:
587 10.1007/s11262-017-1484-5. PubMed PMID: 28664467.
588 34. Ling J, Smura T, Tamarit D, Huitu O, Voutilainen L, Henttonen H, et al. Evolution and
589 postglacial colonization of Seewis hantavirus with Sorex araneus in Finland. Infection, genetics and
590 evolution : journal of molecular epidemiology and evolutionary genetics in infectious diseases.
591 2018;57:88-97. Epub 2017/11/15. doi: 10.1016/j.meegid.2017.11.010. PubMed PMID: 29133028.
592 35. Lee SH, Kim WK, No JS, Kim JA, Kim JI, Gu SH, et al. Dynamic Circulation and Genetic
593 Exchange of a Shrew-borne Hantavirus, Imjin virus, in the Republic of Korea. Scientific reports.
594 2017;7:44369. Epub 2017/03/16. doi: 10.1038/srep44369. PubMed PMID: 28295052; PubMed
595 Central PMCID: PMCPMC5353647.
596 36. Klempa B. Reassortment events in the evolution of hantaviruses. Virus genes.
597 2018;54(5):638-46. Epub 2018/07/27. doi: 10.1007/s11262-018-1590-z. PubMed PMID: 30047031;
598 PubMed Central PMCID: PMCPMC6153690.
599 37. Guterres A, de Oliveira RC, Fernandes J, Maia RM, Teixeira BR, Oliveira FCG, et al. Co-

600 circulation of Araraquara and Juquitiba Hantavirus in Brazilian Cerrado. Microbial ecology.
601 2018;75(3):783-9. Epub 2017/09/01. doi: 10.1007/s00248-017-1061-4. PubMed PMID: 28856421.
602 38. Nikolic V, Stajkovic N, Stamenkovic G, Cekanac R, Marusic P, Siljic M, et al. Evidence of
603 recombination in Tula virus strains from Serbia. Infection, genetics and evolution : journal of
604 molecular epidemiology and evolutionary genetics in infectious diseases. 2014;21:472-8. doi:
605 10.1016/j.meegid.2013.08.020. PubMed PMID: 24008094.
606 39. Sironen T, Vaheri A, Plyusnin A. Molecular evolution of Puumala hantavirus. J Virol.
607 2001;75(23):11803-10. doi: 10.1128/JVI.75.23.11803-11810.2001. PubMed PMID: 11689661;
608 PubMed Central PMCID: PMCPMC114766.
609 40. Chare ER, Gould EA, Holmes EC. Phylogenetic analysis reveals a low rate of homologous
610 recombination in negative-sense RNA viruses. The Journal of general virology. 2003;84(Pt
611 10):2691-703. Epub 2003/09/19. doi: 10.1099/vir.0.19277-0. PubMed PMID: 13679603.
612 41. Wu W, Guo JQ, Yin ZH, Wang P, Zhou BS. GIS-based spatial, temporal, and space-time
613 analysis of haemorrhagic fever with renal syndrome. Epidemiol Infect. 2009;137(12):1766-75. doi:
614 10.1017/S0950268809002659. PubMed PMID: 19393118.
615 42. Zhang WY, Wang LY, Liu YX, Yin WW, Hu WB, Magalhaes RJ, et al. Spatiotemporal
616 transmission dynamics of hemorrhagic fever with renal syndrome in China, 2005-2012. PLoS Negl
617 Trop Dis. 2014;8(11):e3344. doi: 10.1371/journal.pntd.0003344. PubMed PMID: 25412324;
618 PubMed Central PMCID: PMCPMC4239011.
619 43. Wang DM, Wang ZX, Tong YB, Liu M, Cai XH, Hu LJ, et al. [Surveillance on hemorrhagic fever

620 with renal syndrome in Guizhou during 1984-2000]. Zhonghua liu xing bing xue za zhi = Zhonghua
621 liuxingbingxue zazhi. 2003;24(8):694-6. Epub 2003/10/03. PubMed PMID: 14521790.
622 44. Wang ZX. [Preliminary study on epidemic hemorrhagic fever (EHF) in Guizhou Province].
623 Zhonghua liu xing bing xue za zhi = Zhonghua liuxingbingxue zazhi. 1989;10(1):1-5. Epub
624 1989/02/01. PubMed PMID: 2567626.
625 45. Hille A, Tarkhnishvili D, Meinig H, Hutterer R. Morphometric, biochemical and molecular traits
626 in Caucasian wood mice (podemus/Sylvaemus), with remarks on species divergence. Acta
627 Theriologica. 2002;47(4):389-416. doi: 10.1007/bf03192465.
628 46. Liu X, Wei F, Li M, Jiang X, Feng Z, Hu J. Molecular phylogeny and taxonomy of wood mice
629 (genus Apodemus Kaup, 1829) based on complete mtDNA cytochrome b sequences, with
630 emphasis on Chinese species. Molecular phylogenetics and evolution. 2004;33(1):1-15. Epub
631 2004/08/25. doi: 10.1016/j.ympev.2004.05.011. PubMed PMID: 15324834.
632 47. Chen HX, Qiu FX. Epidemiologic surveillance on the hemorrhagic fever with renal syndrome
633 in China. Chinese medical journal. 1993;106(11):857-63. Epub 1993/11/01. PubMed PMID:
634 7908258.
635 48. Klein SL, Calisher CH. Emergence and Persistence of Hantaviruses. In: Childs JE, Mackenzie
636 JS, Richt JA, editors. Wildlife and Emerging Zoonotic Diseases: The Biology, Circumstances and
637 Consequences of Cross-Species Transmission. Berlin, Heidelberg: Springer Berlin Heidelberg;
638 2007. p. 217-52.
639 49. Ramsden C, Holmes EC, Charleston MA. Hantavirus Evolution in Relation to Its Rodent and

640 Insectivore Hosts : No Evidence for Codivergence. 2008. doi: 10.1093/molbev/msn234.

641 50. Souza WM, Bello G, Amarilla AA, Alfonso HL, Aquino VH, Figueiredo LTM. Phylogeography

642 and evolutionary history of rodent-borne hantaviruses. INFECTION, GENETICS AND EVOLUTION.

643 2014;21:198-204. doi: 10.1016/j.meegid.2013.11.015.

644 51. Nemirov K, Henttonen H, Vaheri A, Plyusnin A. Phylogenetic evidence for host switching in

645 the evolution of hantaviruses carried by Apodemus mice. Virus research. 2002;90(1-2):207-15.

646 Epub 2002/11/30. doi: 10.1016/s0168-1702(02)00179-x. PubMed PMID: 12457975.

647 52. Hughes AL, Robert F. Evolutionary Diversification of Protein-Coding Genes of Hantaviruses.

648 Molecular Biology & Evolution. 2000;(10):10.

649 53. Jackson AP, Charleston MA. A cophylogenetic perspective of RNA-virus evolution. Mol Biol

650 Evol. 2004;21(1):45-57. Epub 2003/09/02. doi: 10.1093/molbev/msg232. PubMed PMID:

651 12949128.

652 54. Zhang WY, Guo WD, Fang LQ, Li CP, Bi P, Glass GE, et al. Climate variability and

653 hemorrhagic fever with renal syndrome transmission in Northeastern China. Environmental health

654 perspectives. 2010;118(7):915-20. Epub 2010/02/10. doi: 10.1289/ehp.0901504. PubMed PMID:

655 20142167; PubMed Central PMCID: PMCPMC2920909.

656 55. Clement J, Vercauteren J, Verstraeten WW, Ducoffre G, Barrios JM, Vandamme A-M, et al.

657 Relating increasing hantavirus incidences to the changing climate: the mast connection.

658 International Journal of Health Geographics. 2009;8(1):1. doi: 10.1186/1476-072X-8-1.

659 56. Tian HY, Yu PB, Luis AD, Bi P, Cazelles B, Laine M, et al. Changes in rodent abundance and

660 weather conditions potentially drive hemorrhagic fever with renal syndrome outbreaks in Xi'an,

661 China, 2005-2012. PLoS Negl Trop Dis. 2015;9(3):e0003530. doi: 10.1371/journal.pntd.0003530.

662 PubMed PMID: 25822936; PubMed Central PMCID: PMCPMC4378853.

663 57. McCarthy M. Global climate is warming rapidly, US draft report warns. BMJ. 2017;358:j3824.

664 doi: 10.1136/bmj.j3824. PubMed PMID: 28794049.

665 58. Tian H, Yu P, Cazelles B, Xu L, Tan H, Yang J, et al. Interannual cycles of Hantaan virus

666 outbreaks at the human-animal interface in Central China are controlled by temperature and rainfall.

667 Proc Natl Acad Sci U S A. 2017;114(30):8041-6. doi: 10.1073/pnas.1701777114. PubMed PMID:

668 28696305; PubMed Central PMCID: PMCPMC5544290.

Table S1. Log Marginal Likelihoods computed by Path Sampling and Stepping Stone Sampling

671

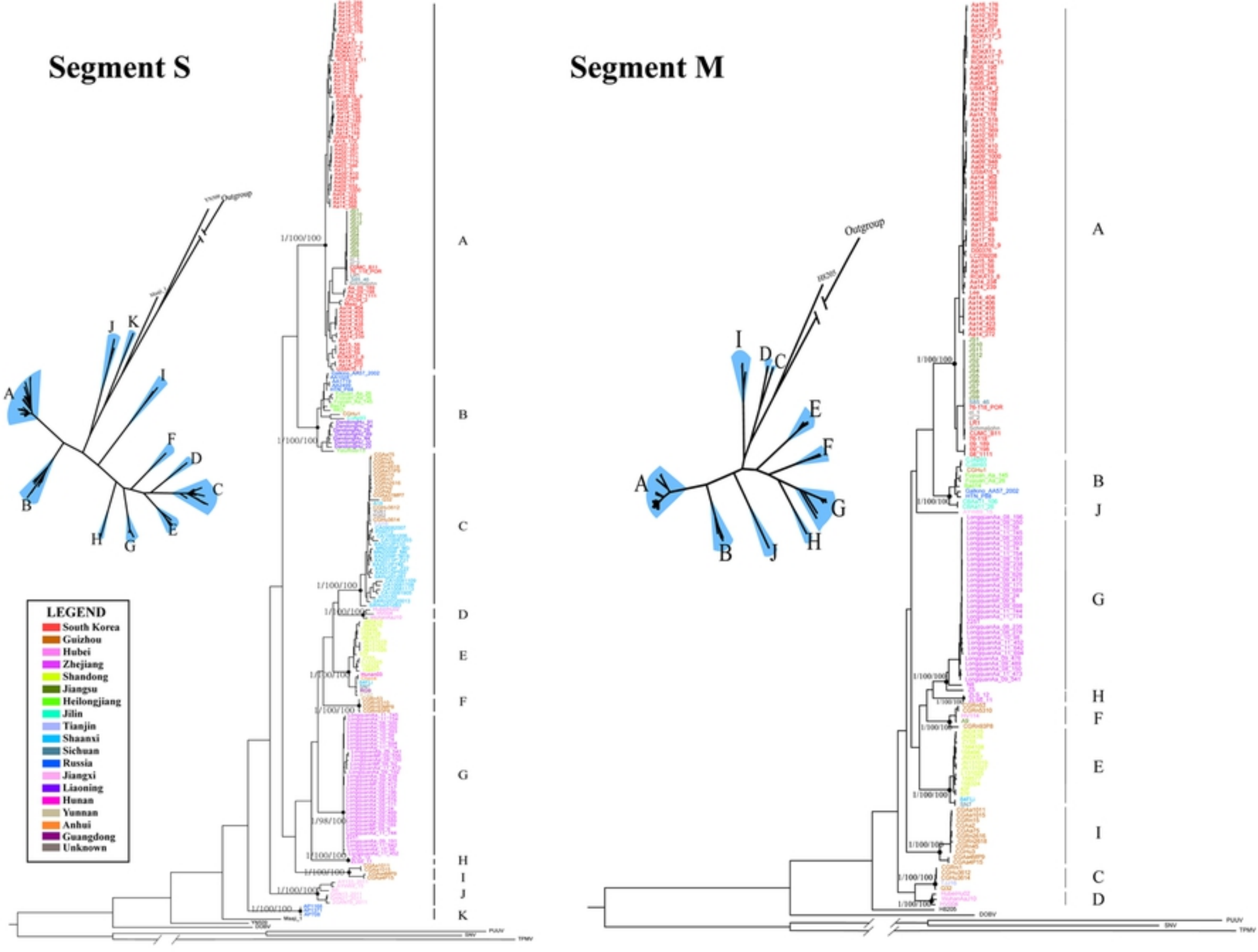
Segment S
Segment M
Outgroup
A
B
C
D
E
F
G
H
I
J
K
LEGEND
South Korea
Guizhou
Hubei
Zhejiang
Shandong
Jiangsu
Heilongjiang
Jilin
Tianjin
Shaanxi
Sichuan
Russia
Jiangxi
Liaoning
Hunan
Yunnan
Anhui
Guangdong
Unknown
DOBV
PUUV
SNV
TPMV

Figure2

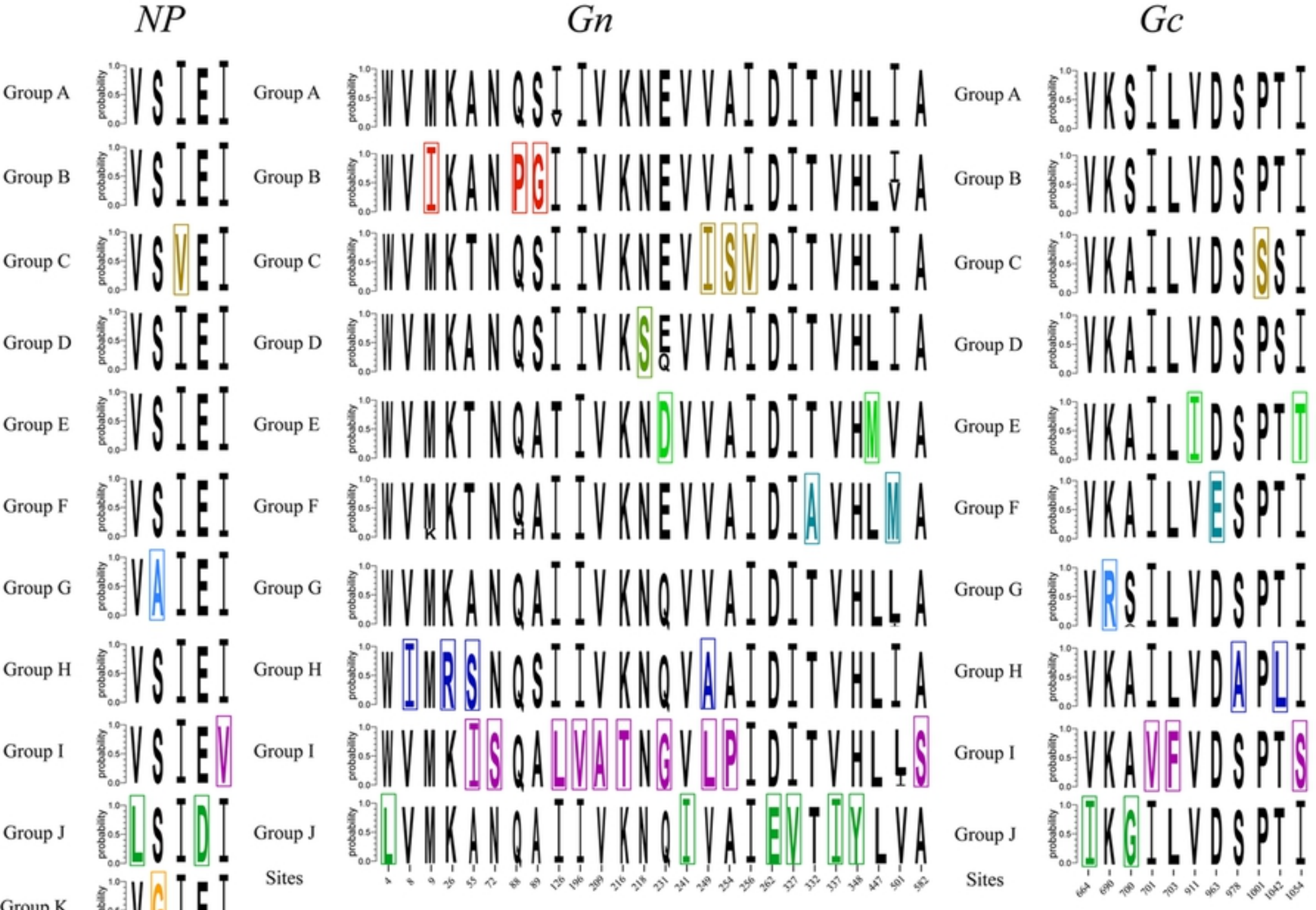
NP
Gn
Gc
Group A
Group B
Group C
Group D
Group E
Group F
Group G
Group H
Group I
Group J
Group K
Sites
179 233 296 297 334
4 8 9 26 55 72 88 89 126 196 289 216 218 231 241 249 254 256 262 327 332 337 348 447 501 582
664 690 700 701 703 911 963 978 1001 1042 1054
probability

Figure3

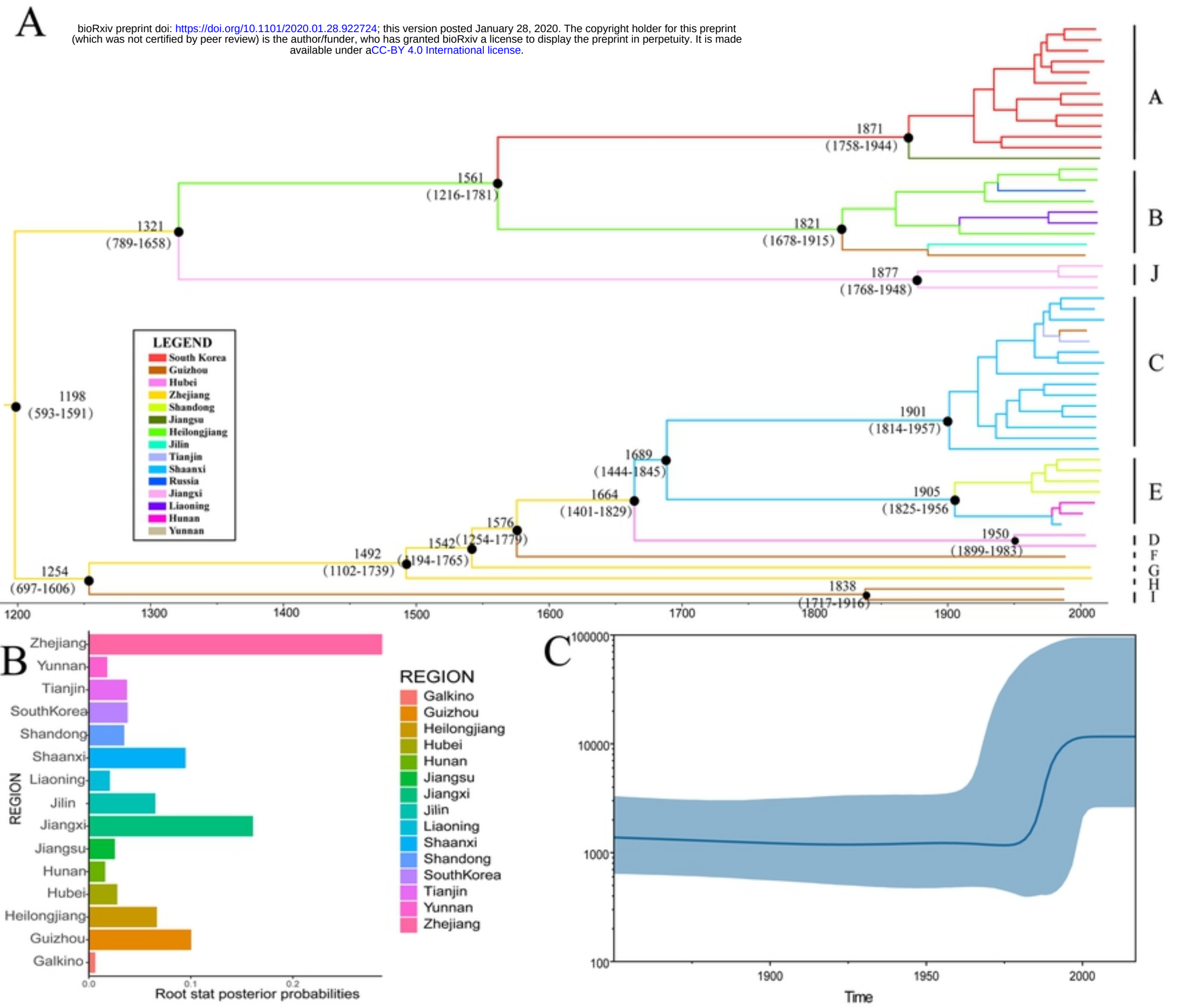

Figure4

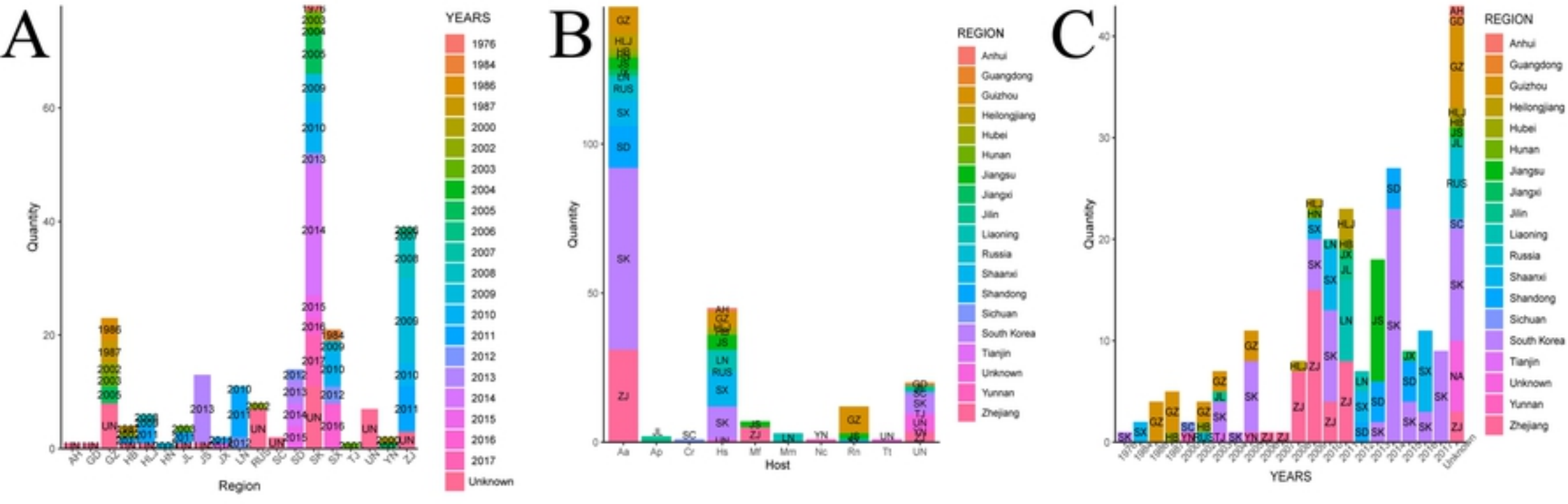
A
Quantity
Region
YEARS
1976
1984
1986
1987
2000
2002
2003
2004
2005
2006
2007
2008
2009
2010
2011
2012
2013
2014
2015
2016
2017
Unknown
B
Quantity
Host
REGION
Anhui
Guangdong
Guizhou
Heilongjiang
Hubei
Hunan
Jiangsu
Jiangxi
Jilin
Liaoning
Russia
Shaanxi
Shandong
Sichuan
South Korea
Tianjin
Unknown
Yunnan
Zhejiang
C
Quantity
YEARS
REGION
Anhui
Guangdong
Guizhou
Heilongjiang
Hubei
Hunan
Jiangsu
Jiangxi
Jilin
Liaoning
Russia
Shaanxi
Shandong
Sichuan
South Korea
Tianjin
Unknown
Yunnan
Zhejiang

Figure

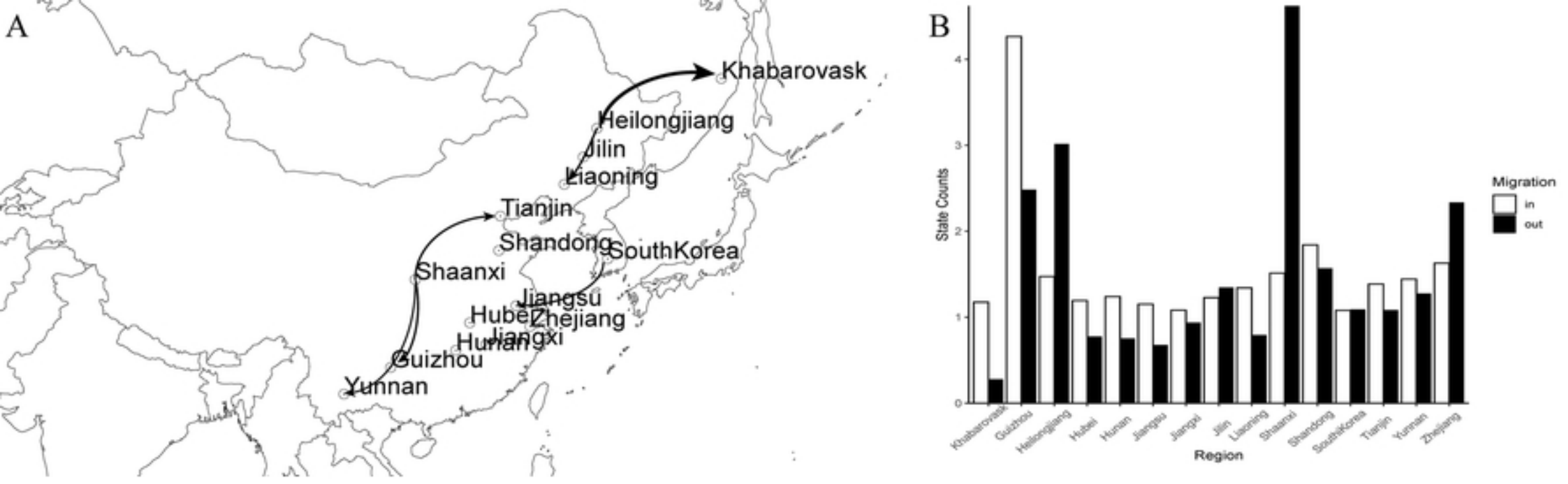
A
Khabarovask
Heilongjiang
Jilin
Liaoning
Tianjin
Shandong
SouthKorea
Shaanxi
Jiangsu
Hubei
Zhejiang
Jiangxi
Hunan
Guizhou
Yunnan
B
State Counts
0
1
2
3
4
Migration
in
out
Khabarovask
Guizhou
Heilongjiang
Hubei
Hunan
Jiangsu
Jiangxi
Jilin
Liaoning
Shaanxi
Shandong
SouthKorea
Tianjin
Yunnan
Zhejiang
Region

Figure